Removal of Spent Nanocomposites Sorbents by Magnetic Separation

Makarchuk O and Dontsova T*

Department of Chemistry, National Technical University of Ukraine, Igor Sikorsky KPI, Kyiv, Ukraine

Corresponding author: Dontsova T

✉ dontsova@ua.fm

Department of Chemistry, National Technical University of Ukraine, Igor Sikorsky KPI, Kyiv 03056, Ukraine.

Tel: +38-093-753-66-36

Abstract

Magnetic nanocomposite sorbents on the basis of saponite, palygorskite and spondyle clay with 2-10% of Fe_3O_4 obtained by impregnation method were investigated. Characterization of magnetic nanocomposite sorbents by the method of physical low temperature adsorption-desorption of nitrogen and powder X-ray diffraction is carried out. Magnetic characteristics of magnetic nanocomposites were compared by constructing of magnetization curves. The correlation between the size of crystallites of nanosized magnetic modifier and the magnetic properties of composites found. The magnetic separation process of spent nanocomposites sorbents was investigated in permanent external magnetic field. The effect of magnetizable medium structuring was discovered. The efficiency of magnetic composites application and implementing of magnetic separation in adsorption purification was proven.

Keywords: Magnetic separation; Magnetic characteristics; Spent nanocomposite sorbents; Nanosized magnetic modifier; Magnetite

Introduction

Adsorption purification with a large variety of sorption materials and equipment is a universal method of wastewater treatment [1]. Sorption materials of natural origin, such as clay minerals, today attract more and more attention. Compared to traditional sorbents, clay minerals have a number of advantages, namely a large specific surface area and sorption capacity, mechanical and chemical resistance, low cost [2,3].

However, the application of clay sorbents in industrial scale is currently limited. This is due to the fact that the sorption activity of clay materials is conditioned by their high dispersion, which creates great difficulty in removing of spent sorbent particles from aqueous medium after achievement of sorption equilibrium [1]. Traditional methods of removing of sorbent sludge from purified water such as centrifugation, filtration and deposition are unacceptable in the production scale of wastewater treatment. The magnetic separation method looks promising for deposition of spent highly dispersed sorbent [4].

But, the use of magnetic separation as a method of removing of spent sorbent requires additional adaptation to technology of adsorption purification. This can be achieved by the use of magnetic composite sorbents based on clay matrix and magnetic modifier [5]. The most popular magnetic modifier is nanosized magnetite Fe_3O_4 [6]. Since nanomagnetite refers to soft magnetic

materials the high controllability of magnetic separation of spent nanocomposite sorbent will be ensured.

The mode of deposition of ferromagnetic particles in a magnetic field is determined not only by their size, but also by the magnetic nature of the matrix in which they are stabilized. Thus, most of the clay minerals are paramagnetic and they will be magnetized in the direction of the external magnetic field created by magnetic separator magnets. These features of clay's allow using them as a base material (matrix) for the creation of magnetic composite sorbents [7].

In this paper, it is proposed to combine the adsorption capacity of the clay and the magnetic properties of magnetite in order to obtain an effective adsorbent, the advantage of which is the possibility of removal from aqueous medium by a simple magnetic separation procedure after the establishment of sorption equilibrium.

Materials and Methods

Clay minerals, namely, saponite, palygorskite, spondyle clay (all clays from Ukraine) were selected for the creation of the magnetic composites sorbents (MC). These materials had paramagnetic properties. It made them suitable for creation on their basis of magnetic sorbents. For synthesis of MC the magnetic modifier Fe_3O_4 was used in the form of magnetic fluid obtained

by Elmore method. Clay minerals have affinity to multicharged cations (particularly iron ions Fe^{2+} and Fe^{3+}) that determined by morphological, crystal and chemistry features of clays. Therefore, magnetic composite sorbents based on magnetite in an amount of 2-10% and saponite (MCSp), palygorskite (MCP) and spondyle clay (MCSd) were synthesized by simple impregnation method [8,9].

Structural and sorption characteristics were measured with the Quantachrome Autosorb (Nova 2200e) by the method of physical adsorption-desorption of nitrogen at 77 K. The surface areas were calculated through the Brunauer-Emmett-Teller (BET) equation. The micropore volume Vmicro and the external surface area S_t were identified from the t-plot method. The value of total pore volume V_{total} was estimated from the maximum adsorption at relative pressure close to the saturation pressure. The pore size distribution of mesopore and micropore was determined from the BJH (Barret–Joyner–Halenda) and Dubinin-Radushkevich method, accordingly [8].

The morphologies of the clay and synthesized sorbents were observed using a scanning electron microscope (SEM 106M). Powder X-ray diffraction (XRD) patterns of natural clays, magnetite and composites on their base were received using diffractometer Rigaku Ultima IV, equipped with CuKα radiation (40 kV, 30 mA). Crystallographic Open Database (COD) was applied for phase composition definition of sorbents. Magnetic properties of nanocomposites (specific magnetization σ_S (A·m²/kg); magnetic field strength H_c (A/m); magnetic induction B_r (mT)) were determined by ballistic magnetometer of Steinberg. Magnetic characteristics of magnetic nanocomposites were analyzed by constructing of magnetization curves.

The magnetic separation process was investigated in an aqueous medium in magnetic filter equipped with permanent magnets with an intensity of external magnetic field, which increased in the direction of subsidence of MC particles from 20 to 200 mT, and in the absence of permanent external magnetic field. The efficiency of magnetic separation was determined by the residual concentration of suspended sorbent particles in aqueous medium through 5, 10, 30 and 60 min of magnetic separation by turbidimetric method [9].

Characterization of magnetic nanocomposite sorbents

Magnetic nanocomposite sorbents containing 2-10% of Fe_3O_4 were synthesized by impregnation method on the basis of saponite (MCSp-2, MCSp-4, MCSp-7 and MCSp-10), palygorskite (MCP-2, MCP-4, MCP-7 and MCP-10) and spondyle clay (MCSd-2, MCSd-4, MCSd-7 and MCSd-10). This method was used on the basis of preliminary studies. They showed that composites obtained by this method have better adsorption-magnetic characteristics [10].

According to previous studies clay minerals modified by nanosized magnetite possessed a greater specific sorption capacity relative to pollutants of different genesis (dyes, surfactants and polyphosphates) in 3-6 times compared to native clays and in 6-20 times relative to magnetic fluid [7,11,12]. Maximum sorption capacities of magnetic nanocomposite sorbents on based various clays are summarized in the **Table 1.** As see, the samples of MC with Fe_3O_4 content of 4-7% have the highest sorption activity **(Table 1)**.

Changing the sorption capacity of all MC samples in relation to all pollutants is consistent with the porous structure of composites and native clays. Characteristics of porous structure of the sorbents MCSp and saponite, MCP and palygorskite, MCSd and spondyle clay are presented in **Tables 2-4** respectively. All MC samples had a higher value of specific surface area and the twice smaller diameter of mesopores than nature clay minerals. The porous structure of magnetite is not shown, since it is known that magnetite is a non-porous sorbent [5].

The comparative analysis of MC samples containing Fe_3O_4

Table 1 Maximal sorption capacities of MC relative to pollutants of different genesis.

Sorbents	Malachite green	Congo red	Sodium dodecyl benzene-sulfonate	Sodium lauryl sulfate	Sodium tripoly-phosphate	Sodium hexameta-phosphate
	Sorption capacity, mg/g					
Saponite	98.94	30.71	8.14	5.19	237.96	279.57
MCSp-2	16.07	73.23	31.91	28.67	498.60	616.84
MCSp-4	278.79	127.11	35.16	30.24	545.92	710.52
MCSp-7	347.21	179.57	36.24	35.60	573.71	817.95
MCSp-10	227.19	146.97	23.27	24.87	514.37	740.50
Palygorskite	51.47	23.28	11.38	5.19	220.31	286.44
MCP-2	106.20	52.32	28.67	27.55	509.86	649.31
MCP-4	156.43	78.43	40.27	29.34	515.12	770.48
MCP-7	204.24	116.12	47.04	32.02	566.20	789.22
MCP-10	149.41	62.35	21.11	19.50	506.86	671.80
Spondyle clay	60.32	30.73	7.06	4.30	216.93	248.96
MCSd-2	142.38	62.42	24.35	21.29	509.86	664.30
MCSd-4	184.65	111.51	38.40	35.60	537.66	791.72
MCSd-7	147.10	90.74	34.07	29.34	551.18	809.20
MCSd-10	80.04	95.93	22.19	26.66	530.90	734.26
Fe_3O_4	36.71	53.55	8.54	4.86	241.22	260.19

Table 2 Characteristics of the porous structure of MCSp and saponite.

Characteristics	Saponite	MCSp-2	MCSp-4	MCSp-7	MCSp-10
Specific surface area (S, m^2/g)	34.6	53.0	55.8	53.8	69.1
Micropore surface area S$_{micro}$, (m^2/g)	9.6	17.4	18.1	12.2	–
External surface area (S$_{ext}$, m^2/g)	25.1	35.6	37.7	41.7	69.1
Total pore volume (V$_{total}$, cm^3/g)	0.12	0.14	0.15	0.15	0.31
Micropore volume (V$_{micro}$, cm^3/g (%)	0.02 (12.9)	0.01 (6.2)	0.01 (6.3)	0.01 (4.4)	–
Mesopore volume (V$_{meso}$, cm^3/g (%)	0.03 (24.7)	0.11 (77.0)	0.11 (78.2)	0.12 (82.7)	0.29 (94.1)
Average pore (diameter d, nm)	12.00	10.39	10.0	10.56	17.66
Average micropore (diameter d, nm)	1.72	0.92	0.91	0.90	0.74
Average mesopore (diameter d, nm)	8.23	4.28	4.35	4.30	12.60

Table 3 Characteristics of the porous structure of MCP and palygorskite.

Characteristics	Palygorskite	MCP-2	MCP-4	MCP-7	MCP-10
Specific surface area (S, m^2/g)	73.0	86.2	81.1	81.8	84.3
Micropore surface area S$_{micro}$, (m^2/g)	24.1	28.3	25.4	22.6	23.5
External surface area (S$_{ext}$, m^2/g)	48.9	57.9	55.8	59.2	60.8
Total pore volume (V$_{total}$, cm^3/g)	0.15	0.17	0.18	0.19	0.21
Micropore volume (V$_{micro}$, cm^3/g (%)	0.01 (8.2)	0.01 (8.5)	0.01 (7.6)	0.01 (5.7)	0.01 (5.8)
Mesopore volume (V$_{meso}$, cm^3/g (%)	0.11 (73.8)	0.12 (74.6)	0.14 (76.7)	0.15 (80.1)	0.14 (65.1)
Average pore (Diameter d, nm)	14.65	7.36	8.39	9.04	19.20
Average micropore diameter d, (nm)	3.33	1.66	1.81	1.93	3.47
Average mesopore diameter d, (nm)	7.66	4.30	4.32	4.32	7.69

Table 4 Characteristics of the porous structure of MCSd and spondyle clay.

Characteristics	Spondyle clay	MCSd-2	MCSd-4	MCSd-7	MCSd-10
Specific surface area (S, m^2/g)	23.7	28.9	33,6	30,8	37.4
Micropore surface area (S$_{micro}$, m^2/g)	5.9	8.2	7,9	7,3	5.2
External surface area (S$_{ext}$, m^2/g)	17.5	20.8	25,7	23,5	32.2
Total pore volume (V$_{total}$, cm^3/g)	0.09	0.08	0,0970	0,0840	0.12
Micropore volume (V$_{micro}$, cm^3/g (%)	0.003 (3.4)	0.004 (4.8)	0,0040 (4,12)	0,0040 (4,76)	0.003 (2.5)
Mesopore volume (V$_{meso}$, cm^3/g (%)	0.044 (50.0)	0.052 (61.9)	0,0683 (70,41)	0,0563 (67,02)	0.067 (56.6)
Average pore (Diameter d, nm)	15.67	11.98	11,84	11,40	13.08
Average micropore diameter d, (nm)	1.86	1.77	1,79	1,77	1.77
Average mesopore (diameter d, nm)	7.54	3.80	3,77	3,80	7.60

in amount of 2-7% indicated an increase of specific surface area due to the development of mesoporous structure during formation of modifier layer on surface of clay matrix pores. As a result of modification, the mesopor content in sorbents based on saponite, palygorskite and spondyle clay increased in 1.5-3.5 times. The average diameter of mesopores and micropores of MC samples was 3.8-4.3 nm and 0.9-1.93 nm, respectively.

For samples of MC, containing 10% magnetite, the specific surface area was decreased due to the blocking of microporous and mesoporous mineral structures. These samples were characterized by pores with an average radius of 9-12 nm, which is explained by the filling of the macroporous structure of clay matrix by magnetic modifier and formation of a secondary porous structure.

Most effective sorbents which were characterized by the most developed porous structure MCSp-7, MCP-7 and MCSd-4 were analyzed by scanning electron microscopy and XRD method.

Figure 1 exposes the SEM micrographs of all nanocomposite sorbents. These images prove the development of mesoporosity in the selected composites.

The XRD pattern of MC samples and native clay minerals are presented in **Figure 2**. The XRD pattern of the native saponite **(Figure 2)** indicated peaks that correspond to saponite (card No. 00-013-0305), montmorillonite (card No. 00-002-0014), quartz (card No. 00-001-0649), calcite (card No. 00-002-0623). The X-ray diffraction pattern of composite sorbents MCSp-7 **(Figure 2)** showed well-developed diffraction lines assigned to inherent phases of native saponite clay, with all major peaks matching the standard pattern of Fe$_3$O$_4$ (card No. 01-071-6336).

A broad diffraction peaks attributed to 2-theta of pure palygorskite (card No. 01-082-1872) and quartz (card No. 00-001-0649) were demonstrated on the XRD pattern of palygorskite **(Figure 2)**. The characteristic diffraction peaks of this two main phases were observed in diffraction pattern of magnetic composites MCP-7. The position of the rest diffraction peaks of MCP samples diffraction pattern were well matched with data from the COD card for Fe$_3$O$_4$ **(Figure 1)**.
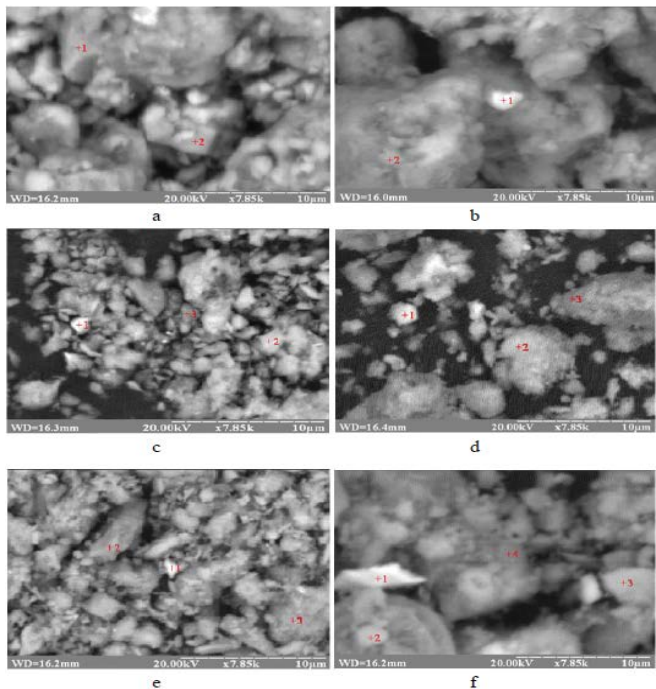
Figure 1   SEM mages of the samples surface: saponite (a), MCSp-7 (b), palygorskite (c), MCP-7 (d), spondyle clay (e) and MCSd-4 (f).

According to the X-ray diffraction analysis presented spondyle clay consists of two minerals such as augite (card No. 01-088-0831) and pigeonite (card No. 01-087-0693). Phase composition of samples MCSd-4 differs from native spondyle clay by the presence of magnetite peaks, which are identified in the **(Figure 2)**.

spondyle clay (e) and MCSd-4 (f): A – Saponite $NaMg_3[AlSi_3O_{10}]$ $(OH)2 \cdot 4H_2O$; B – Montmorillonite $NaMgAlSiO_2(OH) \cdot H_2O$; C – Quartz SiO_2; D – Calcite $CaCO_3$; E – Palygorskite $(Mg_{0.669}, Al_{0.331})$ $4(Si_4O_{10})2(OH)2 \cdot 8H_2O$; F – Augite $Ca(Mg, Fe, Al)[(Si, Al)_2O_6]$; G – Pigeonite $(Ca, Mg, Fe)(Mg, Fe)Si_2O_6$; M – magnetite Fe_3O_4.

The diffraction patterns of MC samples and magnetite had been automatically analyzed by the PDXL software using the international crystallographic data bases PDF-2 and COD. The size of magnetite crystallites in samples MCSp-7, MCP-7 and MCSd-4 was 7.4 nm, 5.0 nm and 4.9 nm, respectively. Also in previous studies it was found, with an increase of magnetite amount introduced into the mineral matrix, the size of its crystallites was increased in the range from 2 nm to 10 nm, and the crystallites size of magnetite in the form of a magnetic fluid was 17.9 nm [9].

Thus, as a result of the synthesis of MC sorbents, the phase composition of various natural sorption materials such as saponite, palygorskite and spondyle clay was preserved and supplemented with nanosized magnetic oxide Fe_3O_4.

Magnetic separation of spent nanocomposite sorbents

Figure 2 presents the magnetization curves of magnetic nanocomposite sorbents of the series MCSp (a), MCP (b), MCSd (c) and Fe_3O_4 (d). As can be seen from **Figure 2,** magnetic

nanocomposites with the same content of magnetic modifier had approximately identical specific magnetization of saturation, which growed in proportion to increase of Fe_3O_4 content in the MC.

Previous studies [9] have shown that with an increase of amount magnetic modifier in the mineral matrix, the size of its crystallites increased. Thus, a significant change of specific saturation magnetization due to the variation of the crystallites size of magnetic modifier by several nanometers was discovered. A comparison of the values obtained size of magnetite crystallites [9], specific magnetization of saturation **(Figure 3)** and coercive force [8,9] shows the following regularities. First, the specific magnetization of saturation and the coercive force of nanosized Fe_3O_4 with crystallite size less than 10 nm proportionally depend on the size of the crystallites. Secondly, magnetite with crystallite size of 17-18 nm has a high value of specific magnetization.
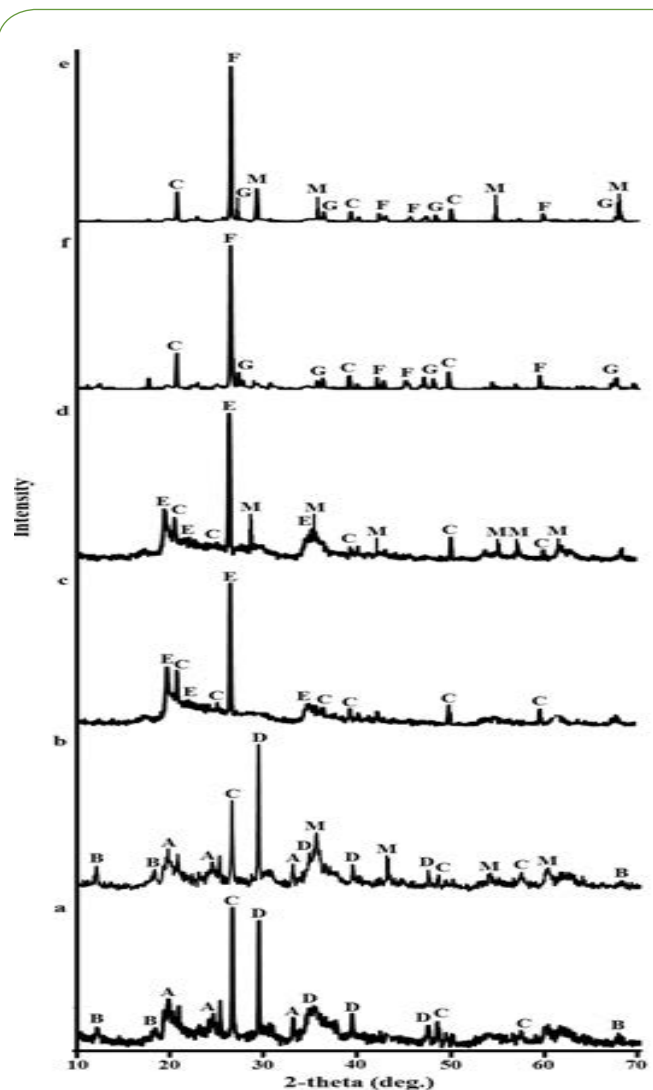

Figure 2   The XRD patterns of saponite (*a*), MCSp-7 (*b*), palygorskite (*c*), MCP-7 (*d*), spondyle clay (*e*) and MCSd-4 (*f*): A – saponite $NaMg_3[AlSi_3O_{10}](OH)_2 \cdot 4H_2O$; B – montmorillonite $NaMgAlSiO_2(OH) \cdot H_2O$; C – quartz SiO_2; D – calcite $CaCO_3$; E – palygorskite $(Mg_{0.669}, Al_{0.331})4(Si_4O_{10})_2(OH)_2 \cdot 8H_2O$; F – augite $Ca(Mg, Fe, Al)[(Si, Al)_2O_6]$; G – pigeonite $(Ca, Mg, Fe)(Mg, Fe)Si_2O_6$; M – magnetite Fe_3O_4.

As an example, for composites with the same magnetite content of 7% such as MCSp-7 and MCP-7 **(Figure 3)**, which have a size of Fe_3O_4 crystallites of 7.4 nm and 5.0 nm, respectively, the specific magnetization saturation was 4.5 $A \cdot m^2/kg$ and 3.9 $A \cdot m^2/kg$, which is consistent among themselves. In addition, the coercive force of these samples was almost identical, about 950 A/m. But, magnetic modifier with the size of crystallites of 17.9 nm was characterized by a higher magnetization of 90 $A \cdot m^2/kg$ at a significantly lower value of coercive force of 501.3 A/m [8,9].

The established regularities are explained by the change in the mechanism of reversal of magnetization from reorientation of magnetic moments (single-domain state) to displacement of domain walls (poly-domain state), which occurred approximately at a crystallite size of 10 nm. Single-domain particles of about the same size had the equal magnetization due to the placement of all spins in one direction. As follows, the process of magnetization of nanosized magnetic modifier with the size of crystallites greater than 10 nm was described by the reversal mechanism of domain walls displacement (poly-domain state). Thus, in the synthesis of nanosized magnetite by the Elmore method and it stabilization on a mineral matrix the nanosized single-domain particles of magnetic material were received.

Discussion

Magnetization curves of MC samples with higher magnetite content have a more rapid course, which means that the magnetic susceptibility and the coercive force are increased

in order MCSp-2<MCSp-4<MCSp-7<MCSp-10, MCP-2<MCP-4<MCP-7<MCP-10 and MCSd-2<MCSd-4<MCSd-7<MCSd-10. The magnetic anisotropy constant is decreased in the listed order.

Magnetic characteristics of MC samples **(Figure 3)** [8,9] and a tendency of increase the crystallite size with increasing of magnetite content in MC samples were compared. It was found that MC with content of magnetite of 10% and biggest one size of crystallite around 10 nm had higher magnetic susceptibility and lower value of the constant of magnetic anisotropy. An intensive magnetization of specimens with content of magnetite of 2-7% was evidently ensured by the high probability of orientation of the vector of spontaneous magnetization in the direction of one of the three possible vectors of easy magnetization due to the matching of crystallite size of a Fe_3O_4 single crystal with size of magnetic domains. Consequently, the magnetic nature of the nanocomposites MC determined by the concentration regime of synthesis and by structural and sorption characteristics of mineral matrix, which stabilized the magnetite of a certain size.

Table 5 shows the kinetic of separation of clay minerals and magnetic composites in external magnetic field and in absence of permanent external magnetic field.

According to the data shown in the **Table 5** the separation of magnetic sorbents from the purified solution in a filter equipped with permanent magnets was held in 36 times faster. 98% of spent magnetic sorbent mass were precipitated for the first 5 minutes by magnetic separation. Application of magnetic composites has ensured the achievement the residual
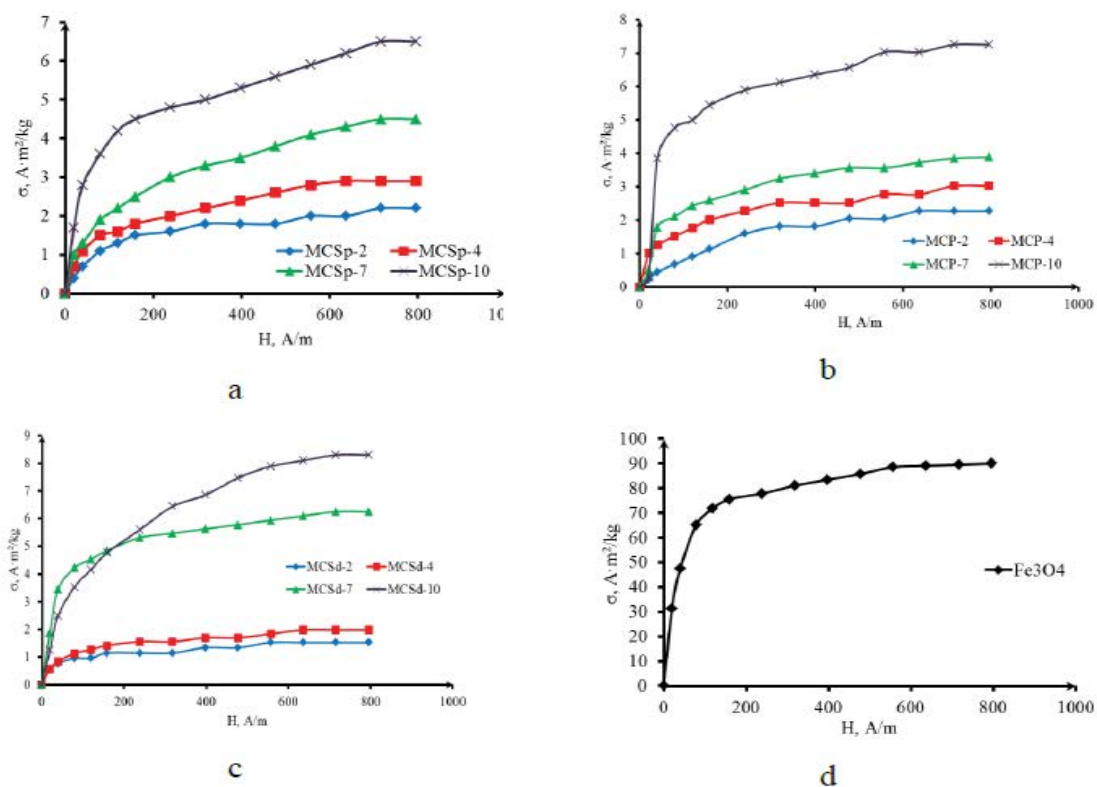

Figure 3 Magnetization curves of nanocomposites MCSp (a), MCP (b), MCSd (c) and Fe_3O_4 (d).

Table 5 Characteristics of the magnetic separation process of spent sorbents.

Samples	20-200 mT				0 mT			
	C (mg/dm³)							
	5 min	10 min	30 min	60 min	5 min	10 min	30 min	60 min
Saponite	558.8	515.4	387.7	327.1	565.7	516.9	388.2	328.0
MCSp-2	252.1	167.1	95.4	58.2	545.4	490.3	364.5	308.4
MCSp-4	121.6	73.2	17.7	14.3	522.9	462.0	328.7	258.3
MCSp-7	32.7	22.7	1.0	<0.5	491.0	458.4	326.6	234.4
MCSp-10	16.6	<0.5	<0.5	<0.5	462.8	418.0	272.6	168.9
MCSp-25	45.4	29.3	24.3	19.3	521.6	503.6	480.7	455.3
MCSp-50	41.6	26.0	9.9	8.8	505.4	472.1	443.8	409.6
Palygorskite	662.7	488.8	418.2	351.6	664.8	487.9	421.3	355.3
MCP-2	209.3	184.9	138.2	71.6	643.5	463.7	381.4	310.2
MCP-4	186.6	148.8	69.3	21.6	618.1	433.6	347.2	272.4
MCP-7	26.6	18.8	<0.5	<0.5	566.5	377.2	285.4	208.2
MCP-10	24.3	<0.5	<0.5	<0.5	498.5	306.8	207.1	124.9
MCP-25	40.6	26.3	18.0	16.5	534.5	517.4	497.0	450.3
MCP-50	34.8	22.4	7.6.	5.9	513.7	488.2	440.1	404.7
Spondyle clay	619.9	573.8	523.2	467.1	617.4	575.4	523.7	466.5
MCSd-2	294.3	179.3	133.2	71.0	601.1	555.7	499.0	438.6
MCSd-4	126.6	43.2	37.1	23.8	585.7	535.2	474.8	410.3
MCSd-7	31.6	23.2	4.9	<0.5	551.0	487.5	412.9	339.3
MCSd-10	21.0	1.56	<0.5	<0.5	517.5	445.8	363.0	281.1
MCSd-25	50.2	38.5	32.7	25.4	559.1	536.4	513.0	486.5
MCSd-50	45.0	29.3	17.4	15.4	520.7	494.1	460.8	421.0

concentration of suspended solids ≤0.02 mg/L for 30 minutes of magnetic separation. Also the residual concentration of magnetic composites was significantly less than native clay sorbents at the separation in the absence of a magnetic field (0 mT).

Herewith modification of cheap clay minerals using nanoscale magnetite in an amount exceeding 10% is economically burdensome. However, for the purpose of more detailed study of magnetic separation process the MC samples containing Fe_3O_4 in amount of 25% and 50% were synthesized. As can be seen from the **Table 5**, sedimentation of the magnetic composite sorbents MCSp-25, MCSp-50, MCP-25, MCP-50, MCSd-25 and MCSd-50 compared to MC samples with content of magnetite of 4-10% was occurred much slower.

The present effect was explained by the structuring of a magnetizable medium in an external magnetic field. MC particles containing nanosized magnetite in excess of 10% turned out to be magnets that magnetized adjacent particles, which, in turn, also created a similar magnetic field of a certain microstructure. Thus, due to the creation by MC particles of a secondary magnetic field that counteracted the primary external magnetic field of permanent magnets a stable macrosystem of a magnetized suspension of composite in an aqueous medium arose. In this case, the precipitation of MC with a magnetite content of more than 10% was caused by aggregation of sorbent particles and their deposition under the influence of gravitational forces. Therefore, magnetic composites are ferromagnetic materials for

which macroscopic magnetic moment, which exists even without external magnetic field, is available. As follows, efficiency of application of magnetic composites and implementing of magnetic separation in adsorption purification is obvious.

Conclusion

Magnetic composite sorbents on mineral base (saponite, palygorskite and spondyle clay) were created by impregnation method. It was proved, that the increase of sorption activity of MC was caused by the decrease of mesopores diameter in two times as a result of nanomagnetite deposition in the porous system of mineral matrix. The specific saturation magnetization of MC samples is consistent with Fe_3O_4 crystallite sizes. It was shown that the change in the mechanism of reversal of magnetization from reorientation of magnetic moments (single-domain state) to displacement of domain walls (poly-domain state) for MC samples was occurred approximately at the magnetite crystallite size of 10 nm.

The removal of spent magnetic sorbents removal took place almost in three times faster compared to native clay and the residual concentration of suspended solids in the water corresponded to standards for drinking water (<0.5 mg/dm³). For magnetic nano-composites with magnetite content of more than 10% the structuring effect of magnetizable medium was revealed. Thus, practical effectiveness of magnetic separation method for the removal of spent magnetic nanocomposite sorbents from the water was confirmed.

References

1   Qin D (2015) Adsorption of ferrous ions onto motmorillonites. Appl Surf Sci 333: 170-177.

2   Rahman A, Urabe T, Kishimoto N (2013) Color removal of reactive procion dyes by clay adsorbents. Procedia Environ Sci 17: 270-278.

3   Gao Y, Chen N, Hu W (2013) Phosphate removal from aqueous solution by an effective clay composite material. J Solution Chem 42: 691-704.

4   Ambashta R, Sillanpaa M (2010) Water purification using magnetic assistance: A review. J of Haza Mater 180: 38-49.

5   Clime L (2008) Magnetic nanocarriers: From material design to magnetic manipulation. Int J Nanitechnol 5(9-12): 1268-1305.

6   Feng L (2012) Superparamagnetic high-surface-area Fe_3O_4 nanoparticlesas adsorbents for arsenic removal. J of Haza Mater 217-218: 439-446.

7   Makarchuk OV, Dontsova TA, Astrelin IM (2016) Magnetic nanocomposites as efficient sorption materials for removing dyes from aqueous solutions. Nanoscale Res Lett 11:161: 1-7.

8   Makarchuk OV, Dontsova TA, Perekos AE (2017) Magnetic nanocomposite sorbents on mineral base. Springer Proceedings in Physics 195: 705-719.

9   Makarchuk OV, Dontsova TA, Perekos AE, Skoblik A, Svystunov Y (2017) Magnetic mineral nanocomposite sorbents for wastewater treatment. J Nanomater 1-7.

10   Makarchuk OV, Dontsova TA, Astrelin IM (2015) Magnetic clay sorbent for the removal of dyes from aqueous solutions. Research Bulletin of the National Technical University of Ukraine Kyiv Polytechnic Institute 6: 109-114.

11   Makarchuk OV, Dontsova TA (2016) Removal of anionic surfactants from wastewater by magnetic mineral sorbents. Journal of water security 2: 1-9.

12   Makarchuk OV, Dontsova TA (2016) Removal of polyphosphates from wastewater by magnetic composite mineral sorbents. European Chemical bulletin 5: 515-523.